Nonperturbative calculation of ZV and ZA in domain-wall QCD on a finite box

doi: 10.1103/PhysRevD.70.034503

Nonperturbative calculation of Z_V and Z_A in domain-wall QCD on a finite box

S. Aoki,[1] M. Fukugita,[2] N. Ishizuka,[1,3] Y. Iwasaki,[1] K. Kanaya,[1] T. Kaneko,[4] Y. Kuramashi,[4] M. Okawa,[5] Y. Taniguchi,[1] A. Ukawa,[1,3] and T. Yoshié[1,3]

(CP-PACS Collaboration)

[1]*Institute of Physics, University of Tsukuba, Tsukuba, Ibaraki 305-8571, Japan*
[2]*Institute for Cosmic Ray Research, University of Tokyo, Kashiwa, Chiba 277-8582, Japan*
[3]*Center for Computational Physics, University of Tsukuba, Tsukuba, Ibaraki 305-8577, Japan*
[4]*High Energy Accelerator Research Organization (KEK), Tsukuba, Ibaraki 305-0801, Japan*
[5]*Department of Physics, Hiroshima University, Higashi-Hiroshima, Hiroshima 739-8526, Japan*

(Received 9 December 2003; published 11 August 2004)

We report on a nonperturbative evaluation of the renormalization factors for the vector and axial-vector currents, Z_V and Z_A, in the quenched domain-wall QCD (DWQCD) with plaquette and renormalization-group-improved gauge actions. We take the Dirichlet boundary condition for both gauge and domain-wall fermion fields on the finite box, and introduce flavor-chiral Ward-Takahashi identities to calculate the renormalization factors. As a test of the method, we numerically confirm the expected relation that $Z_V \simeq Z_A$ in DWQCD. Employing two different box sizes for the numerical simulations at several values of the gauge coupling constant g^2 and the domain-wall height M, we extrapolate Z_V to infinite volume to remove a/L errors. We finally give the interpolation formula of Z_V in the infinite volume as a function of g^2 and M.

DOI: 10.1103/PhysRevD.70.034503 PACS number(s): 11.15.Ha, 11.10.Gh, 11.30.Rd, 12.38.Gc

I. INTRODUCTION

Recent lattice calculations in the domain-wall QCD (DWQCD) have shown that the good chiral property of domain-wall fermions leads to a good scaling behavior of physical observables such as quark masses and B_K [1]. Aside from the quenched approximation, the use of perturbative renormalization factors is the largest source of uncontrolled systematic errors in these calculations. Some kind of nonperturbative renormalization is required to reduce the total error to a few percent level except that from the quenched approximation.

There exist two popular methods for nonperturbative renormalization in lattice QCD: one is the RI-MOM (regularization-independent momentum subtraction) scheme [2], and the other is the SF (Schrödinger functional) scheme [3]. The former method is simpler and has already been applied to DWQCD [4]. The latter one is more suitable to evaluate the scale-dependent renormalization factors. It is rather complicated, however, to implement the SF scheme in DWQCD.

In this paper we formulate a finite volume method very similar to the SF scheme, to calculate the scale-independent renormalization factors Z_V and Z_A. We employ the SF boundary condition for the gauge fields, equivalent to the Dirichlet boundary condition in the absence of boundary fields, while the boundary quark fields with the simple Dirichlet boundary condition, which is different from the SF boundary condition for quarks, are introduced to construct the gauge-invariant observables. In the case of the scale-dependent renormalization factors such as Z_P, an extra perturbative calculation is required to convert the renormalization factors calculated in some scheme with the special boundary condition (ours or the SF) to the one defined in the conventional modified minimal subtraction ($\overline{\mathrm{MS}}$) scheme. In the case of Z_V or Z_A, however, the same renormalization factors are obtained from different boundary conditions, since the flavor-chiral Ward-Takahashi identities uniquely determine them.

Using the finite volume method, we can calculate Z_V and Z_A nonperturbatively at the massless point, so that the systematic error associated with the chiral extrapolation can be removed. The calculation of the scale-independent renormalization factors for vector and axial-vector currents is the first step to the calculation of the scale-dependent renormalization factors for the quark mass and B_K. In addition to this purpose we can use our calculations to probe the chiral symmetry in DWQCD. For example, since chiral symmetry predicts $Z_V = Z_A$, the difference of the two renormalization factors can be used to measure the size of the chiral symmetry breaking in DWQCD.

This paper is organized as follows. In Sec. II we formulate DWQCD on a finite box. In particular we give a detailed description of the quark boundary conditions and explicit forms for the correlation functions which include the boundary quark fields. In Sec. III utilizing the vector an axial-vector Ward-Takahashi identities, we introduce the conditions which determine the renormalization factors for the vector and axial-vector currents. We explicitly give the renormalization factors Z_V and Z_A in terms of the correlation functions on the finite box. In Sec. IV we present results of numerical tests for our method. By investigating the behavior of the quark mass defined through the axial Ward-Takahashi identity as a function of the time, we show that the effect of the Dirichlet boundaries to the zero modes rapidly disappears away from the boundaries. We also show that the expected relation $Z_V \simeq Z_A$ is satisfied for sufficiently large N_s, the size of the fifth dimension of DWQCD. In Sec. V we calculate the renormalization factors at several values of the gauge coupling constant g^2 and the domain-wall height M for both

plaquette and renormalization-group- (RG-) improved gauge actions in the quenched approximation. Using data from two different lattice volumes we extrapolate Z_V to the infinite volume, in order to remove possible $O(a/L)$ errors. We globally fit Z_V in the infinite volume as a function of g^2 and M. Our conclusion and discussion are given in Sec. VI.

II. DWQCD ON A FINITE BOX

A. Gauge action

The gauge action is give by

$$S[U]=\frac{2}{g^2}\left\{c_0\sum_P \mathrm{Re\,tr}(I-U_P)+c_1\sum_R \mathrm{Re\,tr}(I-U_R)\right\},$$

where U_P is the product of the gauge link variables along the plaquette loop P and U_R is the one along the rectangular loop R, with the normalization $c_0+8c_1=1$. Note that the action with $c_1=0$ corresponds to the plaquette action and $c_1=-0.331$ is the RG-improved one obtained by Iwasaki [5].

In the finite volume scheme such as the SF scheme, the theory is defined on $L^3\times T$ lattice with cylinder geometry—i.e., the periodic-type boundary condition (PBC) in the spatial directions and the Dirichlet boundary condition (DBC) in the time direction. Throughout this paper the convention that $L=N_l a$ and $T=N_t a$ is used. In this case the dynamical variables are $U(x)_k$ with times $x_0=a,\ldots,T-a$ and $U(x)_0$ with $x_0=0,\ldots,T-a$ (i.e., inside the cylinder), while Dirichlet boundary conditions are imposed on the fields $U(x)_k$ at $x_0=0$ and T as

$$U(\vec{x},x_0=0)_k=\exp[aC_k],\quad U(\vec{x},x_0=T)_k=\exp[aC'_k],$$

where C_k and C'_k are diagonal matrices [3]:

$$(C_k)_{ij}=\phi_i\delta_{ij},\quad (C'_k)_{ij}=\phi'_i\delta_{ij}.$$

In the calculation of renormalization factors, we take $\phi_i=\phi'_i=0$, zero boundary fields.

In order to remove $O(a)$ errors caused by the DBC, we modify the weights c_0 and c_1 in the action near the boundaries. In the case of the plaquette action the perturbative calculation gives

$$c_0\to c_t=1-0.089g^2-0.030g^4+O(g^6)$$

for each time-space plaquette P_{0k} which just touches one of the boundaries. (The time coordinate for the center of the plaquette $x_0=a/2$ or $T-a/2$.) In the case of the RG action, there exist several choices but we adopt the following one which removes the $O(a)$ term at the tree level [6]:

$$c_1\to\frac{3}{2}c_1$$

for each time-space-space rectangle R_{0kk} which has exactly two lines on a boundary. (Again the time coordinate for the center of the rectangle $x_0=a/2$ or $T-a/2$.) Proof of the $O(a)$ improvement by this choice is given in Ref. [7].

B. Domain-wall fermion on a finite box

The domain-wall fermion action is given by [8]

$$S_F=\overline{\psi}(x,s)D(x,s;y,t)\psi(y,t),$$

where x,y are four-dimensional coordinates and s,t are coordinates in the fifth dimension, which run from 1 to N_s. For the shorthand notation, $X=(x,s)$ and $Y=(y,t)$ are used. Explicitly,

$$D(X,Y)=(5-M)\delta_{XY}-D^4(x,y)\delta_{st}-D^5(s,t)\delta_{xy},$$

$$D^4(x,y)=P_{-\mu}U(x)_\mu\delta_{y,x+\hat{\mu}a}+P_\mu U(y)^\dagger_\mu\delta_{y,x-\hat{\mu}a},$$

$$D^5(s,t)=\begin{cases}P_L\delta_{t,s+1}-m_f P_R\delta_{s,N_s} & (s=1),\\ P_L\delta_{t,s+1}+P_R\delta_{t,s-1} & (1<s<N_s),\\ -m_f P_L\delta_{t,1}+P_R\delta_{t,s-1} & (s=N_s),\end{cases}$$

$$P_{\pm\mu}=\frac{1}{2}(1\pm\gamma_\mu),\quad P_{R/L}=\frac{1}{2}(1\pm\gamma_5).$$

The quark field is defined as usual:

$$q(x)=P_L\psi(x,1)+P_R\psi(x,N_s)\equiv P_L(s)\psi(x,s),$$

$$\overline{q}(x)=\overline{\psi}(x,N_s)P_L+\overline{\psi}(x,1)P_R\equiv\overline{\psi}(x,s)P_R(s),$$

where $P_L(s)=P_L\delta_{s,1}+P_R\delta_{s,N_s}$ and $P_R(s)=P_R\delta_{s,1}+P_L\delta_{s,N_s}$. The following property is useful:

$$[D(x,s;y,t)]^\dagger=\gamma_5 D(y,s^p;x,t^p)\gamma_5,$$

where $s^p=N_s+1-s$, and the dagger here is applied only to color and spinor indices. It is explicitly given by

$$\overline{D(x,s;y,t)^{ba}_{\beta\alpha}}=[\gamma_5 D(y,s^p;x,t^p)^{ab}\gamma_5]_{\alpha\beta},$$

with color indices a,b and spinor indices α,β.

In the finite volume scheme we may rewrite it as

$$\begin{aligned}S_F=&\sum_{a<x_0,y_0<T}\overline{\psi}(x,s)D(x,s;y,t)\psi(y,t)+O(\overline{\rho}\rho,\overline{\rho}'\rho')\\&-\widetilde{c}_t\sum_{x_0=0}[\overline{\psi}(x,s)P_-U(x)_0\psi(x+\hat{0}a,s)\\&+\overline{\psi}(x+\hat{0}a,s)P_+U^\dagger(x)_0\psi(x,s)]\\&-\widetilde{c}_t\sum_{x_0=T}[\overline{\psi}(x-\hat{0}a,s)P_-U(x-\hat{0}a)_0\psi(x,s)\\&+\overline{\psi}(x,s)P_+U^\dagger(x-\hat{0}a)_0\psi(x-\hat{0}a,s)],\end{aligned}\tag{1}$$

with the coefficient $\widetilde{c}_t$ for the boundary counterterm and the boundary condition that

$$\psi(\vec{x},x_0=0,s)=P_+P_L(s)\rho(\vec{x}),$$

$$\overline{\psi}(\vec{x},x_0=0,s)=\overline{\rho}(\vec{x})P_R(s)P_-,$$

$$\psi(\vec{x},x_0=T,s)=P_-P_L(s)\rho'(\vec{x}),$$

$$\overline{\psi}(\vec{x},x_0=T,s)=\overline{\rho'}(\vec{x})P_R(s)P_+,$$

where $P_\pm=P_{\pm 0}$. Terms which contain two external fields are not explicitly written in the first line in Eq. (1), since they do not contribute to the correlation functions we are interested in. Note that this boundary condition is different from the SF boundary condition for quarks [9], since this condition is invariant under the chiral transformation of the domain-wall fermion defined by

$$\psi(x,s)\to e^{iw(s)}\psi(x,s), \tag{2}$$

$$\overline{\psi}(x,s)\to\overline{\psi}(x,s)e^{-iw(s)}, \tag{3}$$

with $w(s)=\theta(s-(N_s+1)/2)$, while the SF boundary condition for quarks must break the chiral symmetry [9]. In the continuum limit the boundary term in the latter case becomes

$$\overline{\psi}(\vec{x},0)P_-\psi(\vec{x},0)+\overline{\psi}(\vec{x},T)P_+\psi(\vec{x},T), \tag{4}$$

which manifestly breaks the chiral symmetry. It may be possible to formulate the domain-wall fermion which satisfies the corresponding SF boundary condition on a cylinder [10].

The classical solution which satisfies the Dirac equation

$$D(X,Y)\psi_{cl}(Y)=0,\quad 0<x_0<T, \tag{5}$$

with boundary values

$$\psi_{cl}(X)|_{x_0=0}=P_+P_L(s)\rho(\vec{x}),$$

$$\psi_{cl}(X)|_{x_0=T}=P_-P_L(s)\rho'(\vec{x}), \tag{6}$$

is given by [11]

$$\psi_{cl}(X)=\tilde{c}_t\sum_Y S(X,Y)[U(y-\hat{0}a)_0^\dagger P_+P_L(t)\rho(\vec{y})|_{y_0=a}+U(y)_0P_-P_L(t)\rho'(\vec{y})|_{y_0=T-a}], \tag{7}$$

where $S(X,Y)$ is the propagator with the zero boundary value:

$$D(X,Y)S(Y,Z)=\delta_{X,Z},\quad 0<x_0<T,$$

$$P_+S(X,Y)|_{x_0=0}=P_-S(X,Y)|_{x_0=T}=S(X,Y)P_-|_{y_0=0}=S(X,Y)P_+|_{y_0=T}=0. \tag{8}$$

Note that the above expression for ψ_{cl} is not valid at $x_0=0$ or T. To show Eq. (5), it is enough to see

$$\begin{aligned}D(X,Y)\psi_{cl}(Y)&=\tilde{c}_t\sum_{Y,0<y_0<T}D(X,Y)\psi_{cl}(Y)\\&\quad+\tilde{c}_t\sum_{Y,y_0=0,T}D(X,Y)\psi_{cl}(Y)\\&=\tilde{c}_t[\,\delta_{x_0,a}U(x-\hat{0}a)_0^\dagger P_+P_L(s)\rho(\vec{x})\\&\quad+\delta_{x_0,T-a}U(x)_0P_-P_L(s)\rho'(\vec{x})|_{x_0=T-a}]\\&\quad-\tilde{c}_t[\,\delta_{x_0,a}P_+U(x-\hat{0}a)_0^\dagger\psi_{cl}(\vec{x},0,s)\\&\quad+\delta_{x_0,T-a}P_-U(x)_0\psi_{cl}(\vec{x},T,s)]=0\end{aligned}$$

for $0<x_0<T$ with boundary values (6). In the actual simulations, the propagator $S(X,Y)$ can be easily obtained by solving the Dirac equation numerically with the condition that $U(\vec{x},x_0=0)_0=U(\vec{x},x_0=T-a)_0=0$.

Now let us consider the path integral for the fermion with source $\eta(x)$, $\overline{\eta}(x)$ and the boundary fields ρ, $\overline{\rho}$, ρ', $\overline{\rho'}$:

$$\begin{aligned}&Z_F(\eta,\overline{\eta},\rho,\overline{\rho},\rho',\overline{\rho'})\\&\quad=\int\mathcal{D}\psi\mathcal{D}\overline{\psi}\exp[-S_F+\overline{\psi}(x,s)P_R(s)\,\eta(x)\\&\qquad+\overline{\eta}(x)P_L(s)\,\psi(x,s)].\end{aligned} \tag{9}$$

To perform the path integration, we introduce the change of variables

$$\psi(x,s)=\psi_{cl}(x,s)+\chi(x,s),\quad \overline{\psi}(x,s)=\overline{\psi}_{cl}(x,s)+\overline{\chi}(x,s),$$

with the boundary condition that $\chi(x,s)=\overline{\chi}(x,s)=0$ at $x_0=0$ and T. Integrating out χ and $\overline{\chi}$ and using the fact that the classical background fields ψ_{cl} and $\overline{\psi}_{cl}$ satisfy the Dirac equation except boundaries, one finally obtains

$$\begin{aligned}Z_F=\det D\exp[&-\overline{\psi}_{cl}(X)D(X,Y)\psi_{cl}(Y)\\&+\overline{\eta}(x)P_L(s)S(X,Y)P_R(t)\,\eta(y)+\overline{\psi}_{cl}(x,s)P_R(s)\,\eta(x)\\&+\overline{\eta}(x)P_L(s)\,\psi_{cl}(x,s)].\end{aligned} \tag{10}$$

Introducing the boundary fields as

$$\zeta(x)=\frac{\vec{\delta}}{\delta\overline{\rho}(x)},\quad \overline{\zeta}(x)=\frac{\vec{\delta}}{\delta\rho(x)},$$

and denoting $q(x)=P_L(s)\psi(x,s)$ and $\overline{q}(x)=\overline{\psi}(x,s)P_R(s)$, we list all fermionic correlation functions used in this paper as follows.

$$\langle q(x)\overline{q}(y)\rangle=\frac{\vec{\delta}}{\delta\overline{\eta}(x)}\log Z_F\frac{\overleftarrow{\delta}}{\delta\eta(y)}=P_L(s)S(X,Y)P_R(t),$$

$$\langle q(x)\overline{\zeta}(y)\rangle = \frac{\vec{\delta}}{\delta\overline{\eta}(x)}\log Z_F \frac{\overleftarrow{\delta}}{\delta\rho(y)} = P_L(s)S(X,Y) \times U(y-\hat{0}a)_0^\dagger P_+ P_L(t)|_{y_0=a},$$

$$\langle \zeta(x)\overline{q}(y)\rangle = P_R(s)P_- U(y-\widehat{0a})_0 S(X,Y)P_R(t)|_{x_0=a} = \gamma_5\langle q(y)\overline{\zeta}(x)\rangle^\dagger\gamma_5,$$

$$\langle q(x)\overline{\zeta'}(y)\rangle = P_L(s)S(X,Y)U(y)_0 P_- P_L(t)|_{y_0=T-a},$$

$$\langle \zeta'(x)\overline{q}(y)\rangle = = P_R(s)P_+ U(y)_0^\dagger S(X,Y)P_R(t)|_{x_0=T-a} \times \gamma_5\langle q(y)\overline{\zeta'}(x)\rangle^\dagger\gamma_5,$$

$$\langle \zeta'(x)\overline{\zeta}(y)\rangle = \frac{\vec{\delta}}{\delta\overline{\rho'}(x)}\log Z_F\frac{\overleftarrow{\delta}}{\delta\rho(y)} = P_R(s)P_+ U(x)_0^\dagger S(X,Y)U(y - \hat{0}a)_0^\dagger P_+ P_L(t)|_{x_0=T-a,y_0=a},$$

$$\langle \zeta(x)\overline{\zeta'}(y)\rangle = P_R(s)P_- U(x-\hat{0}a)_0 S(X,Y) \times U(y)_0 P_- P_L(t)|_{x_0=a,y_0=T-a} = \gamma_5\langle \zeta'(y)\overline{\zeta}(x)\rangle^\dagger\gamma_5, \quad (11)$$

where † is applied to only color and flavor indices.

It is finally noted that the twisted boundary condition in the spatial directions can be imposed for the quarks [3], by replacing

$$U(x)_k \to \lambda_k U(x)_k,$$

where $\lambda_k = e^{ia\theta/L}$.

III. DETERMINATION OF RENORMALIZATION FACTORS

A. Ward-Takahashi identities

The integrated version of Ward-Takahashi (WT) identities are used to determine renormalization factors for vector and axial-vector currents, Z_V and Z_A [3]. Let R be a space-time region with smooth boundary ∂R, and $\mathcal{O}_{\rm int}$ and $\mathcal{O}_{\rm ext}$ are observables localized in the interior and the exterior of R, respectively. The vector WT identity reads

$$\int_{\partial R} d\sigma_\mu(x)\langle [V_\mu^a]^R(x)\mathcal{O}_{\rm int}\mathcal{O}_{\rm ext}\rangle = -\langle(\delta_V^a\mathcal{O}_{\rm int})\mathcal{O}_{\rm ext}\rangle,$$

while the axial-vector WT becomes

$$\int_{\partial R} d\sigma_\mu(x)\langle [A_\mu^a]^R(x)\mathcal{O}_{\rm int}\mathcal{O}_{\rm ext}\rangle = -\langle(\delta_A^a\mathcal{O}_{\rm int})\mathcal{O}_{\rm ext}\rangle + 2m\int_R d^4 \times x\langle [P^a(x)]^R\mathcal{O}_{\rm int}\mathcal{O}_{\rm ext}\rangle,$$

where $[V_\mu^a]^R$ ($[A_\mu^a]^R$) is the renormalized (axial-)vector current and $[P^a]^R$ is the renormalized pseudoscalar density, while unrenormalized quantities are given by

$$V_\mu^a(x) = \overline{q}(x)\gamma_\mu\frac{\tau^a}{2}q(x),$$

$$A_\mu^a(x) = \overline{q}(x)\gamma_\mu\gamma_5\frac{\tau^a}{2}q(x), \quad P^a(x) = \overline{q}(x)\gamma_5\frac{\tau^a}{2}q(x).$$

B. Vector current

We take $R = L^3\times(0,x_0)$, so that ∂R consists of three-dimensional spaces at $t=0$ and at $t=x_0$. As a gauge-invariant observable, we choose $\mathcal{O}_{\rm ext} = \mathcal{O}'^a$ and $\mathcal{O}_{\rm int} = \mathcal{O}^a$ with

$$\mathcal{O}^a = a^6\sum_{\vec{u},\vec{v}}\overline{\zeta}(u)\gamma_5\frac{1}{2}\tau^a\zeta(v),$$

$$\mathcal{O}'^a = a^6\sum_{\vec{u},\vec{v}}\overline{\zeta'}(u)\gamma_5\frac{1}{2}\tau^a\zeta'(v),$$

where τ^a is the Pauli matrix for flavors with $\mathrm{tr}\,\tau^a\tau^b = 2\delta_{ab}$ and $\tau^a\tau^b = \delta^{ab} + i\epsilon^{abc}\tau^b\tau^c$, and ζ and ζ' correspond to our boundary fields. With this choice and

$$\delta_V^a\mathcal{O}^b = -i\epsilon^{abc}\mathcal{O}^c,$$

the vector WT identity gives the relation

$$Z_V(1+b_V m_f a)f_V(x_0) = f_1, \quad (12)$$

where

$$f_V(x_0) = \frac{a^3}{6L^6}\sum_{\vec{x}} i\epsilon^{abc}\langle\mathcal{O}'^a V_0^b(x)\mathcal{O}^c\rangle, \quad (13)$$

$$f_1 = -\frac{1}{3L^3}\langle\mathcal{O}'^a\mathcal{O}^a\rangle. \quad (14)$$

From Eq. (12) we can determine Z_V, the renormalization factor for the vector current, together with the b_V, one of the $O(ma)$ improvement coefficients. Note that $b_V = 0$ if the chiral symmetry of DWQCD is exactly satisfied.

C. Axial-vector current

For the axial-vector current, we take $R = L^3\times(y_0-t, y_0+t)$, $\mathcal{O}_{\rm int} = A_0^b(y_0)$ and

$$\mathcal{O}_{\rm ext} = -\epsilon^{cde}\mathcal{O}'^{d}\mathcal{O}^{e},$$

and plug them into the axial-vector WT identity with $m=0$. We then obtain

$$Z_A^2 f_{AA}^I(y_0,x_0^+,x_0^-) = 2Z_V f_V(y_0) = 2f_1, \tag{15}$$

where

$$f_{AA}^I(y_0,x_0^+,x_0^-) = -\frac{a^6}{6L^6}\sum_{x,y}\epsilon^{abc}\epsilon^{cde}\langle\mathcal{O}'^{d}\{A_0^a(x_0^+,\vec{x}) - A_0^a(x_0^-,\vec{x})\}A_0^b(y)\mathcal{O}^e\rangle, \tag{16}$$

with $x_0^{\pm} = y_0 \pm t$.

We finally define the unrenormalized quark mass $m_{\rm AWTI}$ through the following WT identity:

$$f_A(x_0+a) - f_A(x_0-a) = 4(m_{\rm AWTI}a)f_P(x_0), \tag{17}$$

where

$$f_A(x_0) = -\frac{a^6}{3}\langle A_0^a(x)\mathcal{O}^a\rangle, \quad f_P(x_0) = -\frac{a^6}{3}\langle P^a(x)\mathcal{O}^a\rangle. \tag{18}$$

IV. TEST OF THE FORMULATION BY NUMERICAL SIMULATIONS

A. Effects of boundaries on quark masses

Since the boundary condition in time with $\rho = \overline{\rho} = 0$ is identical to the Shamir's domain-wall (Dirichlet) boundary condition [8], extra zero modes may appear near $x_0 = 0$ and T. One has to check whether these unwanted zero modes induce an extra contribution to the low energy observables at $0 \ll x_0 \ll T$. Here we consider the quark mass $am_{\rm AWTI}$, defined through the axial Ward-Takahashi identity (AWTI). In Fig. 1, we plot $am_{\rm AWTI}$ for free theory as a function of x_0

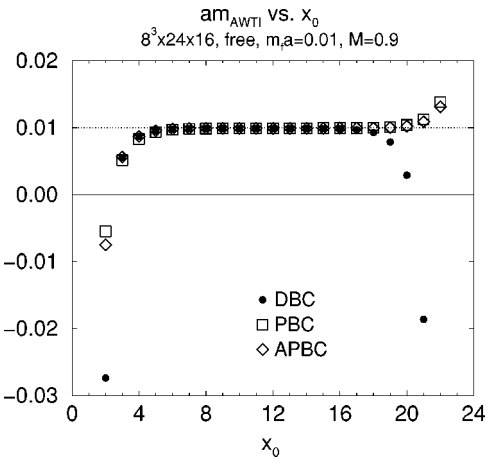

FIG. 1. $am_{\rm AWTI}$ as a function of x_0 with Dirichlet (solid circles), periodic (open squares), and antiperiodic (open diamonds) boundary conditions.

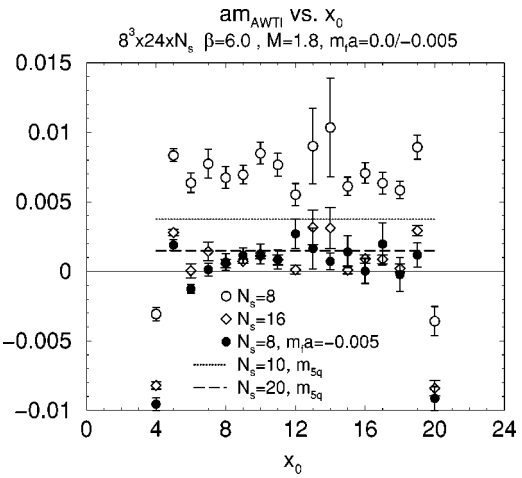

FIG. 2. $am_{\rm AWTI}$ as a function of x_0 at $\beta=6.0$ on an $8^3\times24\times N_s$ lattice at $m_f a=0$ with $N_s=8$ (open circles) and 16 (open diamonds) and at $m_f=-0.005$ with $N_s=8$ (solid circles), together with m_{5q} at $N_s=10$ (dotted line) and $N_s=20$ (dashed line) [12].

with Dirichlet, periodic, and antiperiodic boundary conditions at the bare quark mass $m_f a=0.01$, on an $8^3\times24\times16$ lattice, with the domain-wall height $M=0.9$. The dependence of $am_{\rm AWTI}$ on the boundary condition, which is visible near the boundaries, disappears away from them. Therefore we conclude at least for the free case that the extra zero modes associated with the Dirichlet boundary condition have negligible effects on the determination of the renormalization factors evaluated at $x_0 \simeq T/2$.

In Fig. 2, $am_{\rm AWTI}$ in the quenched DWQCD with our boundary condition is plotted as a function of x_0 on $8^3\times24\times N_s$ lattices with $m_f a=0$ and $M=1.8$ at $\beta=6.0$ for the plaquette gauge action. Since the x_0 dependence is weak away from the boundaries, we nonperturbatively confirm the conclusion in the free case that the effect of the Dirichlet boundary condition is negligible. Interestingly $m_{\rm AWTI}$ is nonzero even at $m_f a=0$, and becomes smaller for larger N_s. Moreover, the value is consistent with m_{5q}, a measure of the explicit chiral symmetry breaking calculated from the conserved axial-vector current of DWQCD [12]. More precisely $m_{\rm AWTI}$ at $m_f a=0$ is equal to $(Z_P/Z_A)m_{5q}$ up to a small lattice artifact. This fact suggests that $m_{\rm AWTI}$ in our finite volume scheme may be a better alternative as the measure of explicit chiral symmetry breaking in DWQCD, since it can be calculated directly at $m_f a=0$ with much less computational cost. Note also that the large explicit breaking in $m_{\rm AWTI}$ at $N_s=8$ (open circles) is compensated for if one takes a negative quark mass of $m_f a=-0.005$ (solid circles). This demonstrates that the domain-wall fermion at $N_s \neq \infty$ can be considered as a highly improved Wilson fermion [13].

For lack of exact chiral symmetry at finite N_s, there is no unique definition for the massless point. In this paper we adopt $m_f a=0$ as our massless point for the calculation of renormalization factors, instead of taking $m_f a=-m_{5q}a$ as usually done for the Wilson fermions. Although differences in renormalization factors between the two definitions exist, they are expected to be sufficiently small at $N_s=16$.

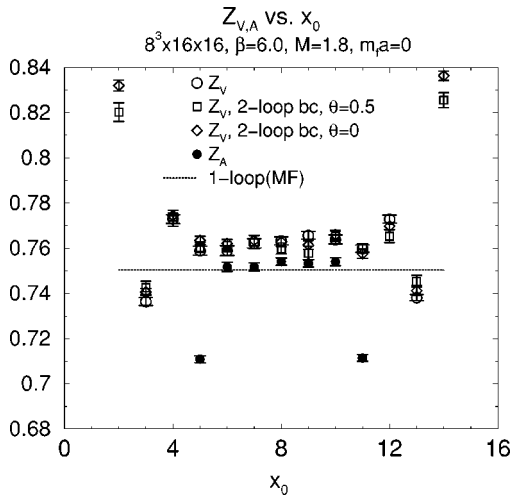

FIG. 3. Z_V and Z_A as a function of x_0 at $\beta=6.0$ on an $8^3\times16\times16$ lattice with $M=1.8$ and $m_f a=0$. We compare the results from the boundary counterterms at the tree level (circles) with those at two loop (squares and diamonds) as well as those at $\theta=0$ with that at $\theta=0.5$ (squares).

B. Renormalization factors

The nonperturbative renormalization factors for vector and axial-vector currents are defined at $m_f a=0$ by the relation that $Z_V=f_1/f_V(x_0)$ and $Z_A^2=2f_1/f_{AA}^I(x_0,x_0^+,x_0^-)$, where we fix $x_0^\pm=T/2\pm T/4$. In this paper we do not attempt to determine b_V, which must vanish exponentially in N_s. In Fig. 3, Z_V and Z_A are plotted as a function of x_0 on $8^3\times16\times16$ at $\beta=6.0$ with $M=1.8$ and $m_f=0$. Similar to the case of am_{AWTI} a plateau is seen away from the boundaries. The relation $Z_V=Z_A$, valid exactly in perturbation theory, is

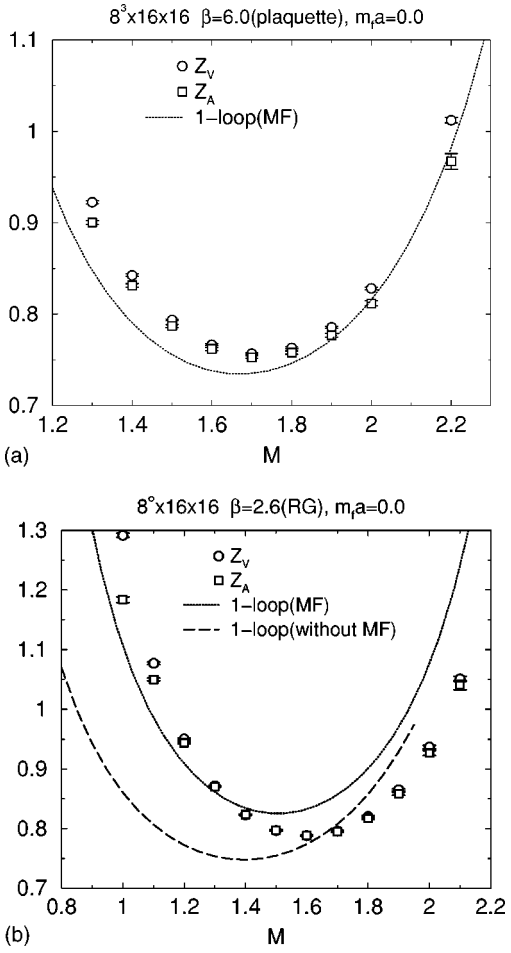

FIG. 4. Z_V and Z_A vs M on $8^3\times16\times16$ at $\beta=6.0$ for plaquette action (upper) and at $\beta=2.6$ for the RG action (lower). Perturbative estimates are given at one loop with the MF improvement (solid lines) and without it (dashed line).

TABLE I. Simulation parameters.

	Plaquette				RG improved		
β	a^{-1}(GeV)	No. of conf.	No. of conf.	β	a^{-1}(GeV)	No. of conf.	No. of conf.
		$8^3\times16\times16$	$4^3\times8\times16$			$8^3\times16\times16$	$4^3\times8\times16$
				2.2	1.0	100	100–200
5.8	1.4	100	100	2.4	1.4	100	100–200
		$8^3\times16\times16$	$12^3\times24\times16$			$8^3\times16\times16$	$12^3\times24\times16$
6.0	2.0	100	20	2.6	1.9	100	30
6.2	2.7	100	10–30	2.9	2.9	100	15–50
6.5	4.1	100	15–25	3.2	4.3	100	20–25
6.8	6.1	100	10–15	3.6	6.8	100	20–25
7.4	12	100	10–20	4.1	12	100	20–25
8.0	25	40	7–15	4.7	23	40	10–20
9.6	156	40	10	6.4	154	40	10–20
12.0	2502	20	10	8.85	2523	20	10–15
24.0	3.2×10^9	20	10	21.0	3.6×10^9	20	10

TABLE II. Results for the plaquette action.

	Z_A	Z_V		Z_V at $L=L^*$			Z_V at $L=\infty$		
M	$8^3\times16$	$8^3\times16$	$4^3\times8$	Z_V^L	Fit	δ_G (%)	Z_V^L	Fit	δ_G (%)
$\beta=5.8$, $a^{-1}=1.4$ GeV, $L^*/a=5.6$									
1.3	0.7724(119)	1.0398(69)	0.9535(78)	1.0028(87)	1.0153	1.2	1.1260(596)	1.1318	0.5
1.4	0.7203(94)	0.9013(37)	0.8603(64)	0.8837(48)	0.8815	0.2	0.9423(290)	0.9406	0.2
1.5	0.6914(104)	0.8179(28)	0.7852(63)	0.8122(33)	0.8062	0.7	0.8313(123)	0.8250	0.8
1.6	0.6603(83)	0.7624(41)	0.7731(90)	0.7670(46)	0.7641	0.4	0.7516(141)	0.7514	0.02
1.7	0.6383(98)	0.7348(30)	0.7659(68)	0.7481(42)	0.7449	0.4	0.7036(226)	0.7046	0.1
1.8	0.6377(82)	0.7245(30)	0.7711(41)	0.7444(45)	0.7443	0.01	0.6778(319)	0.6768	0.1
1.9	0.6309(79)	0.7238(42)	0.7939(134)	0.7538(85)	0.7624	1.1	0.6537(493)	0.6641	1.6
2.0	0.6290(84)	0.7330(55)	0.8550(129)	0.7853(118)	0.8029	2.2	0.6110(831)	-	-
2.1	0.6710(115)	0.7894(54)	0.9848(122)	0.8732(171)	0.8755	0.3	0.5940(1313)	-	-
2.2	0.6722(149)	0.8660(81)	1.2024(160)	1.0102(287)	1.0037	0.6	0.5296(2254)	-	-
2.3	0.7080(203)	1.0079(106)	1.8025(796)	1.3484(736)	1.2499	7.3	0.2132(5361)	-	-
$\beta=6.0$, $a^{-1}=2.0$ GeV, $L^*/a=8.0$									
1.3	0.9002(21)	0.9252(30)	0.9308(36)	0.9252(30)	0.9253	0.01	0.9421(141)	0.9438	0.2
1.4	0.8330(21)	0.8446(25)	0.8472(32)	0.8446(25)	0.8431	0.2	0.8526(112)	0.8491	0.4
1.5	0.7884(20)	0.7950(22)	0.7927(44)	0.7950(22)	0.7935	0.2	0.7656(227)	0.7885	3.0
1.6	0.7633(19)	0.7674(21)	0.7635(50)	0.7674(21)	0.7666	0.1	0.7555(163)	0.7511	0.6
1.7	0.7541(19)	0.7572(21)	0.7438(42)	0.7572(21)	0.7578	0.1	0.7169(208)	0.7316	2.0
1.8	0.7589(20)	0.7628(21)	0.7439(35)	0.7628(21)	0.7659	0.4	0.7062(254)	0.7272	3.0
1.9	0.7781(23)	0.7852(21)	0.7761(43)	0.7852(21)	0.7921	0.9	0.7577(175)	0.7375	3.0
2.0	0.8153(30)	0.8300(25)	0.8044(58)	0.8300(25)	0.8406	1.3	0.7532(356)	0.7636	1.4
2.1	0.8802(52)	0.9179(34)	0.8647(84)	0.9179(34)	0.9210	0.3	0.7583(690)	0.8092	6.7
2.2	0.9941(95)	1.0706(48)	0.9722(81)	1.0706(48)	1.0535	1.6	0.7754(1209)	-	-
$\beta=6.2$, $a^{-1}=2.7$ GeV, $L^*/a=10.8$									
1.2	0.9734(15)	0.9896(21)	0.9899(25)	0.9898(20)	0.9926	0.3	0.9904(87)	0.9982	0.8
1.3	0.8858(11)	0.8937(14)	0.8911(19)	0.8917(15)	0.8921	0.04	0.8859(70)	0.8947	1.0
1.4	0.8294(07)	0.8321(13)	0.8242(18)	0.8260(15)	0.8295	0.4	0.8084(113)	0.8284	2.5
1.5	0.7957(10)	0.7969(16)	0.7915(32)	0.7927(25)	0.7923	0.1	0.7805(121)	0.7872	0.9
1.6	0.7764(09)	0.7781(13)	0.7700(27)	0.7718(21)	0.7744	0.3	0.7537(129)	0.7651	1.5
1.7	0.7766(10)	0.7778(14)	0.7693(28)	0.7712(23)	0.7731	0.2	0.7524(135)	0.7589	0.9
1.8	0.7892(11)	0.7949(18)	0.7918(21)	0.7925(17)	0.7884	0.5	0.7855(82)	0.7681	2.2
1.9	0.8196(14)	0.8319(19)	0.8190(23)	0.8219(19)	0.8223	0.05	0.7932(174)	0.7936	0.05
2.0	0.8659(27)	0.8908(22)	0.8734(30)	0.8772(24)	0.8802	0.3	0.8386(231)	0.8389	0.04
$\beta=6.5$, $a^{-1}=4.1$ GeV, $L^*/a=16.4$									
1.1	1.0458(13)	1.0656(18)	1.0689(26)	1.0707(42)	1.0635	0.7	1.0757(95)	1.0588	1.6
1.2	0.9416(10)	0.9469(16)	0.9480(19)	0.9485(31)	0.9449	0.4	0.9500(67)	0.9431	0.7
1.3	0.8715(08)	0.8728(13)	0.8698(16)	0.8682(26)	0.8700	0.2	0.8638(65)	0.8690	0.6
1.4	0.8285(08)	0.8290(12)	0.8256(16)	0.8238(27)	0.8236	0.02	0.8188(68)	0.8226	0.5
1.5	0.8042(06)	0.8042(11)	0.8024(11)	0.8014(19)	0.7981	0.4	0.7987(47)	0.7966	0.3
1.6	0.7963(07)	0.7976(08)	0.7939(23)	0.7919(36)	0.7898	0.3	0.7864(84)	0.7876	0.2
1.7	0.8051(07)	0.8082(12)	0.8031(14)	0.8004(23)	0.7976	0.3	0.7930(77)	0.7945	0.2
1.8	0.8246(10)	0.8335(14)	0.8279(23)	0.8249(38)	0.8226	0.3	0.8167(101)	0.8181	0.2
1.9	0.8687(17)	0.8853(17)	0.8797(26)	0.8767(41)	0.8682	1.0	0.8685(108)	0.8615	0.8
2.0	0.9345(29)	0.9730(21)	0.9531(25)	0.9424(52)	0.9419	0.1	0.9132(254)	0.9311	2.0

TABLE II. (*Continued*).

	Z_A	Z_V		Z_V at $L=L^*$			Z_V at $L=\infty$		
M	$8^3\times16$	$8^3\times16$	$4^3\times8$	Z_V^L	Fit	δ_G (%)	Z_V^L	Fit	δ_G (%)
$\beta=6.8$, $a^{-1}=6.1$ GeV, $L^*/a=24.4$									
1.2	0.9250(07)	0.9250(13)	0.9233(13)	0.9215(31)	0.9211	0.03	0.9198(52)	0.9192	0.1
1.3	0.8667(07)	0.8656(12)	0.8647(19)	0.8638(41)	0.8610	0.3	0.8629(64)	0.8605	0.3
1.4	0.8317(06)	0.8304(10)	0.8269(20)	0.8232(43)	0.8250	0.2	0.8197(75)	0.8253	0.7
1.5	0.8156(06)	0.8157(09)	0.8085(19)	0.8011(49)	0.8078	0.8	0.7940(105)	0.8088	1.9
1.6	0.8140(07)	0.8147(12)	0.8141(14)	0.8134(31)	0.8070	0.8	0.8129(49)	0.8088	0.5
1.7	0.8300(07)	0.8359(10)	0.8319(11)	0.8279(30)	0.8227	0.6	0.8239(63)	0.8253	0.2
1.8	0.8575(11)	0.8692(14)	0.8685(13)	0.8677(31)	0.8568	1.3	0.8670(50)	0.8603	0.8
1.9	0.9116(19)	0.9393(16)	0.9271(17)	0.9147(63)	0.9142	0.1	0.9027(158)	0.9189	1.8
$\beta=7.4$, $a^{-1}=12$ GeV, $L^*/a=48$									
1.1	0.9761(06)	0.9762(11)	0.9744(14)	0.9717(41)	0.9693	0.2	0.9708(53)	0.9677	0.3
1.2	0.9090(07)	0.9078(09)	0.9054(12)	0.9019(37)	0.9005	0.2	0.9007(48)	0.9002	0.1
1.3	0.8646(05)	0.8631(08)	0.8642(14)	0.8658(37)	0.8582	0.9	0.8663(45)	0.8588	0.9
1.4	0.8437(05)	0.8441(08)	0.8398(16)	0.8335(53)	0.8359	0.3	0.8313(72)	0.8376	0.8
1.5	0.8394(05)	0.8403(08)	0.8374(13)	0.8332(41)	0.8309	0.3	0.8318(54)	0.8337	0.2
1.6	0.8497(05)	0.8535(08)	0.8504(23)	0.8457(63)	0.8424	0.4	0.8442(80)	0.8467	0.3
1.7	0.8748(07)	0.8854(09)	0.8829(20)	0.8792(55)	0.8718	0.8	0.8780(69)	0.8782	0.02
1.8	0.9150(14)	0.9418(11)	0.9375(10)	0.9311(43)	0.9232	0.8	0.9289(63)	0.9325	0.4
$\beta=8.0$, $a^{-1}=25$ GeV, $L^*/a=100$									
0.9	1.1644(16)	1.1842(22)	1.1814(20)	1.1764(73)	1.1674	0.8	1.1757(82)	1.1669	0.8
1.0	1.0421(08)	1.0437(13)	1.0431(14)	1.0383(49)	1.0340	0.4	1.0378(55)	1.0337	0.4
1.1	0.9578(08)	0.9575(12)	0.9538(10)	0.9471(51)	0.9486	0.2	0.9462(60)	0.9485	0.2
1.2	0.9031(07)	0.9024(09)	0.8972(17)	0.8881(71)	0.8946	0.7	0.8868(83)	0.8948	0.9
1.3	0.8715(05)	0.8712(10)	0.8674(11)	0.8607(51)	0.8634	0.3	0.8598(60)	0.8640	0.5
1.4	0.8576(06)	0.8565(09)	0.8542(09)	0.8501(37)	0.8506	0.1	0.8495(43)	0.8520	0.3
1.5	0.8601(06)	0.8615(11)	0.8600(07)	0.8575(32)	0.8548	0.3	0.8572(36)	0.8572	0.0
1.6	0.8790(08)	0.8846(14)	0.8846(11)	0.8847(40)	0.8763	0.9	0.8847(44)	0.8802	0.5
1.7	0.9164(11)	0.9341(10)	0.9284(19)	0.9186(78)	0.9180	0.1	0.9172(91)	0.9241	0.8
1.8	0.9738(21)	1.0074(18)	0.9979(14)	0.9812(105)	0.9860	0.5	0.9789(127)	0.9953	1.7
$\beta=9.6$, $a^{-1}=156$ GeV, $L^*/a=624$									
0.9	1.0897(07)	1.0921(11)	1.0855(08)	1.0726(83)	1.0787	0.6	1.0723(86)	1.0817	0.9
1.0	0.9994(06)	0.9973(09)	0.9947(09)	0.9897(43)	0.9892	0.1	0.9896(44)	0.9901	0.1
1.1	0.9412(05)	0.9395(07)	0.9356(07)	0.9279(52)	0.9324	0.5	0.9278(54)	0.9322	0.5
1.2	0.9053(05)	0.9032(09)	0.9016(05)	0.8984(30)	0.8995	0.1	0.8983(31)	0.8986	0.03
1.3	0.8895(05)	0.8884(07)	0.8876(06)	0.8859(25)	0.8858	0.01	0.8859(25)	0.8847	0.1
1.4	0.8928(06)	0.8938(10)	0.8926(11)	0.8903(40)	0.8899	0.05	0.8903(41)	0.8887	0.2
1.5	0.9129(04)	0.9181(07)	0.9154(08)	0.9099(41)	0.9120	0.2	0.9098(42)	0.9112	0.2
1.6	0.9471(08)	0.9621(09)	0.9605(12)	0.9573(44)	0.9551	0.2	0.9572(44)	0.9550	0.2
1.7	1.0023(17)	1.0362(12)	1.0319(10)	1.0236(63)	1.0253	0.2	1.0235(64)	1.0266	0.3
1.8	1.0946(32)	1.1568(17)	1.1425(18)	1.1145(178)	1.1346	1.8	1.1139(183)	1.1383	2.2

satisfied nonperturbatively within 1%–2%.[1] Moreover, the magnitude of $Z_{V,A}$ almost agrees with the value at one loop in the mean-field- (MF-) improved perturbation theory using the plaquette [14]. We also observe that Z_V is insensitive to boundary parameters such as the two-loop boundary counterterms for gauge fields and the parameter θ of the twisted boundary condition for quarks.

C. Dependence of $Z_{V,A}$ on M

We calculate Z_V and Z_A in the quenched DWQCD at $a^{-1}\simeq 2$ GeV with the plaquette action ($\beta=6.0$) and with the RG-improved action ($\beta=2.6$) on an $8^3\times16\times16$ lattice with $m_f a=0$ for $M=1.0$–2.2. The results are summarized in Fig. 4, where Z_V and Z_A are plotted as a function of M, together

[1]Note however that a small difference between Z_V and Z_A is beyond the statistical errors. This small difference is expected to vanish exponentially as $N_s\to\infty$.

TABLE II. (*Continued*).

	Z_A	Z_V		Z_V at $L=L^*$			Z_V at $L=\infty$		
M	$8^3\times16$	$8^3\times16$	$4^3\times8$	Z_V^L	Fit	δ_G (%)	Z_V^L	Fit	δ_G (%)
$\beta=12.0$, $a^{-1}=2502$ GeV, $L^*/a=10008$									
0.7	1.2733(14)	1.3174(18)	1.3131(14)	1.3043(76)	1.2946	0.7	1.3043(76)	1.3051	0.1
0.8	1.1437(07)	1.1500(12)	1.1461(09)	1.1383(59)	1.1370	0.1	1.1383(60)	1.1418	0.3
0.9	1.0467(06)	1.0440(10)	1.0411(06)	1.0356(44)	1.0364	0.1	1.0355(44)	1.0381	0.2
1.0	0.9803(06)	0.9759(10)	0.9747(04)	0.9724(26)	0.9723	0.01	0.9724(26)	0.9720	0.04
1.1	0.9405(04)	0.9369(06)	0.9346(09)	0.9301(39)	0.9341	0.4	0.9301(39)	0.9326	0.3
1.2	0.9200(03)	0.9179(05)	0.9170(05)	0.9151(22)	0.9166	0.2	0.9151(22)	0.9142	0.1
1.3	0.9202(06)	0.9199(07)	0.9181(05)	0.9145(31)	0.9175	0.3	0.9145(31)	0.9145	0.0
1.4	0.9360(05)	0.9391(07)	0.9372(03)	0.9332(29)	0.9370	0.4	0.9332(29)	0.9336	0.04
1.5	0.9685(06)	0.9806(09)	0.9772(08)	0.9705(50)	0.9776	0.7	0.9705(50)	0.9738	0.3
1.6	1.0200(14)	1.0473(14)	1.0456(03)	1.0423(39)	1.0448	0.2	1.0423(39)	1.0408	0.1
1.7	1.1011(30)	1.1572(12)	1.1501(08)	1.1360(91)	1.1500	1.2	1.1359(92)	1.1460	0.9
1.8	1.2299(54)	1.3400(20)	1.3202(15)	1.2805(245)	1.3150	2.7	1.2805(246)	1.3114	2.4
$\beta=24.0$, $a^{-1}=3.2\times10^9$ GeV, $L^*/a=1.28\times10^{10}$									
0.5	1.4168(27)	1.5526(11)	1.5441(05)	1.5272(106)	1.5323	0.3	1.5272(106)	1.5406	0.9
0.6	1.2735(09)	1.3079(07)	1.3063(04)	1.3030(27)	1.3003	0.2	1.3030(27)	1.3043	0.1
0.7	1.1603(02)	1.1604(05)	1.1597(06)	1.1583(21)	1.1565	0.2	1.1583(21)	1.1582	0.01
0.8	1.0746(03)	1.0669(04)	1.0662(03)	1.0647(14)	1.0644	0.03	1.0647(14)	1.0647	0.0
0.9	1.0154(03)	1.0083(05)	1.0069(04)	1.0040(22)	1.0064	0.2	1.0040(22)	1.0059	0.2
1.0	0.9802(03)	0.9752(04)	0.9738(03)	0.9710(20)	0.9738	0.3	0.9710(20)	0.9725	0.2
1.1	0.9666(02)	0.9629(03)	0.9619(02)	0.9600(15)	0.9619	0.2	0.9600(15)	0.9602	0.02
1.2	0.9716(02)	0.9696(03)	0.9693(02)	0.9685(09)	0.9695	0.1	0.9685(09)	0.9673	0.1
1.3	0.9946(03)	0.9976(04)	0.9969(02)	0.9956(13)	0.9974	0.2	0.9956(13)	0.9947	0.1
1.4	1.0350(03)	1.0493(06)	1.0485(02)	1.0468(17)	1.0492	0.2	1.0468(17)	1.0461	0.1
1.5	1.0959(08)	1.1324(06)	1.1316(04)	1.1300(19)	1.1328	0.2	1.1300(19)	1.1290	0.1
1.6	1.1820(23)	1.2638(06)	1.2615(04)	1.2571(32)	1.2630	0.5	1.2571(32)	1.2584	0.1
1.7	1.3151(40)	1.4815(07)	1.4698(08)	1.4464(143)	1.4706	1.7	1.4464(143)	1.4647	1.3

with one-loop perturbative estimates with and without MF improvement [14]. For both gauge actions, $Z_V \simeq Z_A$ holds, and they have a minimum at $M \simeq 1.7$ for the plaquette action or $M \simeq 1.6$ for the RG action. The deviation from $Z_V = Z_A$ becomes larger as M goes far away from the minimum. Perturbative estimates without MF improvement fail, particularly for the plaquette action for which the curve can not be placed in the figure. The MF improvement makes the agreement much better for both actions.

V. RESULTS

We extract Z_V and Z_A at various values of g^2 for both plaquette- and RG-improved gauge actions on an $N_l^3\times N_t \times N_s = 8^3\times16\times16$ lattice. In addition we employ a different four-dimensional lattice size $N_l^3\times N_t = 12^3\times24$ or $4^3\times8$, while keeping $N_s=16$, in order to investigate the $a/L = 1/N_l$ dependences of Z_V and Z_A. Simulation parameters are given in Table I, together with the lattice spacing a, obtained from the global parametrization for the string tension as a function of g^2:

$$\sigma^{1/2}a = a(g^2)\frac{1+c_2\hat{a}^2(g^2)+c_4\hat{a}^4(g^2)+c_6\hat{a}^6(g^2)}{c_0}, \tag{19}$$

$$a(g^2) = (b_0 g^2)^{-b_1}\exp\left[-\frac{1}{2b_0 g^2}\right], \tag{20}$$

$$\hat{a}(g^2) = \frac{a(g^2)}{a(g_0^2)}, \tag{21}$$

where $b_0 = 11/(4\pi)^2$ and $b_1 = 102/(4\pi)^4$ (the coefficients of β function in the quenched theory). The coefficients of the parametrization become $c_0 = 0.01364$, $c_2 = 0.2731$, $c_4 = -0.01545$, and $c_6 = 0.01975$, with $g_0^2 = 1.0$ for the plaquette action [15], and $c_0 = 0.524$, $c_2 = 0.274$, $c_4 = 0.105$, and $c_6 = 0$, with $g_0^2 = 6/2.4$ for the RG action [16]. We use $\sigma^{1/2} = 0.44$ GeV to get a in Table I. Gauge fields are updated bythe pseudo-heat-bath algorithm with five hits, followed by four overrelaxation sweeps; the combination of these updates is called an iteration. After 2000 iterations for a thermalization, we calculate the fermionic correlation functions on the gauge configurations separated by 200 iterations. On each M at given β, different gauge configurations are used to evaluate Z_V and Z_A, so that the measurements of Z's at different M are independent. Raw data of Z_V (the third and fourth columns) and Z_A (the second column) are compiled in Table II for the plaquette action and Table III for the RG action.

TABLE III. Results for the RG action.

	Z_A	Z_V		Z_V at $L=L^*$			Z_V at $L=\infty$		
M	$8^3\times16$	$8^3\times16$	$4^3\times8$	Z_V^L	Fit	δ_G (%)	Z_V^L	Fit	δ_G (%)
$\beta=2.2$, $a^{-1}=1.0$ GeV, $L^*/a=4.0$									
1.3	0.4365(102)	1.1434(62)	0.9888(121)	0.9888(121)	1.0170	2.9	1.2980(1045)	1.2608	2.9
1.4	0.4588(109)	0.9356(55)	0.8746(136)	0.8746(136)	0.8671	0.9	0.9967(443)	1.0040	0.7
1.5	0.4438(95)	0.8356(51)	0.8160(104)	0.8160(104)	0.7934	2.8	0.8552(196)	0.8575	0.3
1.6	0.4489(108)	0.7693(59)	0.7741(89)	0.7741(89)	0.7553	2.4	0.7646(151)	0.7667	0.3
1.7	0.4429(95)	0.7336(41)	0.7701(81)	0.7701(81)	0.7388	4.1	0.6970(270)	0.7089	1.7
1.8	0.4661(181)	0.7165(51)	0.7429(93)	0.7429(93)	0.7388	0.6	0.6901(223)	0.6732	2.4
1.9	0.4580(109)	0.7086(49)	0.7664(119)	0.7664(119)	0.7553	1.4	0.6507(415)	0.6540	0.5
2.0	0.4615(130)	0.7092(65)	0.8094(162)	0.8094(162)	0.7931	2.0	0.6090(700)	-	-
2.1	0.4516(130)	0.7360(55)	0.8478(282)	0.8478(282)	0.8657	2.1	0.6243(804)	-	-
2.2	0.4533(130)	0.8019(12)	1.0583(401)	1.0583(401)	1.0115	4.4	0.5437(1778)	-	-
2.3	0.4641(132)	0.8787(14)	1.5012(463)	1.5012(463)	1.3809	8.0	0.2562(4185)	-	-
$\beta=2.4$, $a^{-1}=1.4$ GeV, $L^*/a=5.6$									
1.1	0.9735(137)	1.2773(65)	1.1902(116)	1.2400(94)	1.2486	0.7	1.3644(606)	1.32455	2.9
1.2	0.9350(90)	1.0415(57)	1.0109(84)	1.0284(55)	1.0319	0.3	1.0721(248)	1.07925	0.7
1.3	0.8645(66)	0.9193(43)	0.9151(85)	0.9175(44)	0.9084	1.0	0.9235(124)	0.93494	1.2
1.4	0.8143(52)	0.8438(41)	0.8348(78)	0.8399(41)	0.8343	0.7	0.8527(128)	0.84436	1.0
1.5	0.7680(37)	0.7887(40)	0.8020(141)	0.7944(65)	0.7911	0.4	0.7753(185)	0.78675	1.5
1.6	0.7508(44)	0.7654(39)	0.7877(157)	0.7749(73)	0.7700	0.6	0.7430(230)	0.75191	1.2
1.7	0.7441(39)	0.7615(42)	0.7898(50)	0.7736(39)	0.7675	0.8	0.7333(212)	0.73465	0.2
1.8	0.7546(51)	0.7636(37)	0.8137(92)	0.7851(61)	0.7832	0.2	0.7135(354)	0.73266	2.7
1.9	0.7613(52)	0.7787(36)	0.8405(119)	0.8052(74)	0.8195	1.8	0.7170(434)	0.74565	4.0
2.0	0.7859(90)	0.8219(45)	0.9342(130)	0.8701(110)	0.8832	1.5	0.7096(765)	-	-
2.1	0.8461(143)	0.8969(49)	1.0704(175)	0.9712(163)	0.9888	1.8	0.7234(1174)	-	-
2.2	0.8927(238)	1.0406(116)	1.4389(650)	1.2113(433)	1.1692	3.5	0.6423(2744)	-	-
2.3	0.9352(487)	1.3270(183)	2.3382(2358)	1.7604(1309)	1.5119	14.1	0.3157(7151)	-	-
$\beta=2.6$, $a^{-1}=1.9$ GeV, $L^*/a=7.6$									
1.0	1.1837(49)	1.2926(41)	1.3479(75)	1.2839(53)	1.2828	0.1	1.4586(706)	1.3310	8.7
1.1	1.0498(23)	1.0772(27)	1.1013(55)	1.0734(33)	1.0729	0.04	1.1495(338)	1.1012	4.2
1.2	0.9440(15)	0.9496(19)	0.9663(41)	0.9469(24)	0.9482	0.1	0.9999(239)	0.9634	3.7
1.3	0.8706(10)	0.8703(15)	0.8737(33)	0.8698(19)	0.8706	0.1	0.8806(112)	0.8763	0.5
1.4	0.8235(08)	0.8217(14)	0.8228(21)	0.8215(17)	0.8233	0.2	0.8250(71)	0.8210	0.5
1.5	0.7973(08)	0.7951(15)	0.7933(28)	0.7953(18)	0.7977	0.3	0.7899(92)	0.7884	0.2
1.6	0.7882(09)	0.7861(17)	0.7880(29)	0.7858(20)	0.7900	0.5	0.7918(95)	0.7735	2.3
1.7	0.7947(12)	0.7932(20)	0.7860(45)	0.7943(24)	0.7992	0.6	0.7715(167)	0.7746	0.4
1.8	0.8171(16)	0.8172(24)	0.8072(41)	0.8188(29)	0.8264	0.9	0.7872(178)	0.7917	0.6
1.9	0.8585(24)	0.8626(31)	0.8538(98)	0.8640(40)	0.8757	1.4	0.8364(318)	0.8270	1.1
2.0	0.9267(41)	0.9408(43)	0.9136(36)	0.9451(51)	0.9559	1.1	0.8591(355)	-	-
2.1	1.0403(78)	1.0816(67)	1.0086(90)	1.0932(83)	1.0846	0.8	0.8625(927)	-	-
$\beta=2.9$, $a^{-1}=2.9$ GeV, $L^*/a=11.6$									
1.1	0.9945(12)	1.0002(20)	0.9916(23)	0.9922(21)	0.9909	0.1	0.9743(130)	0.9983	2.5
1.2	0.9124(07)	0.9147(12)	0.9128(16)	0.9129(15)	0.9091	0.4	0.9089(58)	0.9110	0.2
1.3	0.8625(07)	0.8634(09)	0.8583(11)	0.8587(10)	0.8579	0.1	0.8482(72)	0.8558	0.9
1.4	0.8332(08)	0.8336(12)	0.8290(17)	0.8294(16)	0.8289	0.1	0.8199(79)	0.8236	0.5
1.5	0.8223(08)	0.8223(15)	0.8178(15)	0.8181(14)	0.8179	0.02	0.8088(75)	0.8098	0.1
1.6	0.8266(07)	0.8279(10)	0.8231(14)	0.8234(13)	0.8234	0.0	0.8134(75)	0.8125	0.1
1.7	0.8483(08)	0.8519(13)	0.8455(10)	0.8459(10)	0.8461	0.03	0.8327(87)	0.8321	0.1
1.8	0.8878(14)	0.8986(17)	0.8928(16)	0.8932(15)	0.8892	0.5	0.8811(91)	0.8711	1.1
1.9	0.9572(23)	0.9764(20)	0.9569(21)	0.9582(19)	0.9591	0.1	0.9177(246)	0.9353	1.9
2.0	1.0691(48)	1.1059(24)	1.0654(36)	1.0682(34)	1.0691	0.1	0.9846(499)	1.0358	5.2

TABLE III. (*Continued*).

	Z_A	Z_V		Z_V at $L=L^*$			Z_V at $L=\infty$		
M	$8^3\times16$	$8^3\times16$	$4^3\times8$	Z_V^L	Fit	δ_G (%)	Z_V^L	Fit	δ_G (%)
$\beta=3.2$, $a^{-1}=4.3$ GeV, $L^*/a=17.2$									
1.1	0.9649(97)	0.9663(12)	0.9618(13)	0.9591(24)	0.9591	0.0	0.9529(71)	0.9600	0.7
1.2	0.9026(05)	0.9025(11)	0.8991(17)	0.8971(28)	0.8969	0.02	0.8924(68)	0.8951	0.3
1.3	0.8635(06)	0.8631(09)	0.8603(11)	0.8587(19)	0.8595	0.1	0.8549(49)	0.8559	0.1
1.4	0.8453(07)	0.8460(11)	0.8423(12)	0.8400(22)	0.8415	0.2	0.8348(62)	0.8365	0.2
1.5	0.8455(05)	0.8469(09)	0.8421(11)	0.8392(21)	0.8404	0.1	0.8326(68)	0.8346	0.2
1.6	0.8603(07)	0.8626(10)	0.8596(10)	0.8578(18)	0.8562	0.2	0.8535(51)	0.8497	0.4
1.7	0.8939(08)	0.9013(14)	0.8943(11)	0.8901(23)	0.8908	0.1	0.8804(93)	0.8838	0.4
1.8	0.9476(16)	0.9652(13)	0.9583(16)	0.9542(29)	0.9492	0.5	0.9447(97)	0.9417	0.3
1.9	1.0351(25)	1.0708(18)	1.0518(22)	1.0403(52)	1.0408	0.04	1.0138(240)	1.0329	1.9
2.0	1.1747(62)	1.2589(30)	1.2033(33)	1.1697(121)	1.1850	1.3	1.0920(677)	1.1763	7.7
$\beta=3.6$, $a^{-1}=6.8$ GeV, $L^*/a=27.2$									
1.0	1.0210(07)	1.0222(11)	1.0204(16)	1.0183(36)	1.0162	0.2	1.0166(57)	1.0165	0.01
1.1	0.9467(05)	0.9463(08)	0.9418(09)	0.9369(29)	0.9407	0.4	0.9329(62)	0.9389	0.6
1.2	0.8983(05)	0.8975(09)	0.8960(09)	0.8944(22)	0.8937	0.1	0.8931(36)	0.8907	0.3
1.3	0.8730(05)	0.8729(07)	0.8696(09)	0.8660(26)	0.8681	0.2	0.8631(49)	0.8644	0.2
1.4	0.8655(05)	0.8660(07)	0.8637(09)	0.8610(23)	0.8604	0.1	0.8589(41)	0.8566	0.3
1.5	0.8750(05)	0.8781(08)	0.8738(10)	0.8690(31)	0.8697	0.1	0.8652(62)	0.8662	0.1
1.6	0.9007(05)	0.9075(07)	0.9044(10)	0.9010(27)	0.8970	0.4	0.8983(50)	0.8943	0.4
1.7	0.9459(08)	0.9609(09)	0.9547(11)	0.9479(39)	0.9462	0.2	0.9424(83)	0.9449	0.3
$\beta=4.1$, $a^{-1}=12$ GeV, $L^*/a=48$									
1.0	0.9981(05)	0.9972(08)	0.9954(08)	0.9928(28)	0.9920	0.1	0.9919(37)	0.9904	0.2
1.1	0.9381(04)	0.9366(06)	0.9329(07)	0.9273(34)	0.9324	0.6	0.9254(51)	0.9297	0.5
1.2	0.9025(04)	0.9016(06)	0.8979(06)	0.8925(33)	0.8972	0.5	0.8907(49)	0.8941	0.4
1.3	0.8867(04)	0.8865(06)	0.8831(07)	0.8781(31)	0.8815	0.4	0.8764(46)	0.8785	0.2
1.4	0.8880(03)	0.8896(05)	0.8868(07)	0.8824(30)	0.8834	0.1	0.8810(43)	0.8808	0.02
1.5	0.9067(05)	0.9107(09)	0.9076(09)	0.9029(35)	0.9030	0.02	0.9014(50)	0.9014	0.0
1.6	0.9428(06)	0.9531(09)	0.9493(08)	0.9436(38)	0.9429	0.1	0.9417(55)	0.9429	0.1
1.7	1.0003(12)	1.0237(11)	1.0193(12)	1.0127(48)	1.0087	0.4	1.0104(68)	1.0114	0.1
$\beta=4.7$, $a^{-1}=23$ GeV, $L^*/a=92$									
0.9	1.0618(06)	1.0626(10)	1.0614(11)	1.0592(36)	1.0554	0.4	1.0589(41)	1.0543	0.4
1.0	0.9854(06)	0.9836(09)	0.9810(09)	0.9766(37)	0.9784	0.2	0.9760(44)	0.9762	0.02
1.1	0.9364(05)	0.9351(08)	0.9306(05)	0.9229(47)	0.9305	0.8	0.9217(58)	0.9278	0.7
1.2	0.9100(06)	0.9096(07)	0.9054(05)	0.8981(45)	0.9048	0.7	0.8970(55)	0.9020	0.6
1.3	0.9011(05)	0.9015(08)	0.9002(06)	0.8980(26)	0.8977	0.04	0.8976(30)	0.8953	0.3
1.4	0.9119(05)	0.9143(07)	0.9111(10)	0.9057(41)	0.9083	0.3	0.9048(49)	0.9067	0.2
1.5	0.9394(05)	0.9466(07)	0.9419(08)	0.9337(52)	0.9381	0.5	0.9325(63)	0.9377	0.6
1.6	0.9862(11)	1.0010(12)	0.9981(06)	0.9929(40)	0.9909	0.2	0.9922(48)	0.9926	0.04
1.7	1.0542(19)	1.0903(15)	1.0844(14)	1.0742(73)	1.0748	0.1	1.0727(87)	1.0799	0.7
$\beta=6.4$, $a^{-1}=154$ GeV, $L^*/a=616$									
0.8	1.1139(05)	1.1146(08)	1.1116(07)	1.1057(43)	1.1081	0.2	1.1056(44)	1.1072	0.1
0.9	1.0288(05)	1.0248(07)	1.0238(06)	1.0217(25)	1.0219	0.02	1.0217(26)	1.0203	0.1
1.0	0.9740(04)	0.9711(05)	0.9696(04)	0.9666(24)	0.9678	0.1	0.9666(24)	0.9658	0.1
1.1	0.9426(03)	0.9405(04)	0.9381(03)	0.9334(30)	0.9375	0.4	0.9333(31)	0.9356	0.2
1.2	0.9311(03)	0.9300(06)	0.9277(94)	0.9233(31)	0.9271	0.4	0.9232(32)	0.9254	0.2
1.3	0.9385(03)	0.9396(05)	0.9382(04)	0.9354(23)	0.9352	0.02	0.9353(23)	0.9339	0.1
1.4	0.9624(03)	0.9674(05)	0.9665(05)	0.9647(20)	0.9629	0.2	0.9647(21)	0.9623	0.2
1.5	1.0056(06)	1.0194(07)	1.0169(07)	1.0119(39)	1.0136	0.2	1.0118(40)	1.0143	0.3
1.6	1.0746(12)	1.1034(09)	1.1005(11)	1.0950(48)	1.0950	0.0	1.0949(50)	1.0978	0.3

TABLE III. (*Continued*).

	Z_A	Z_V		Z_V at $L=L^*$			Z_V at $L=\infty$		
M	$8^3\times16$	$8^3\times16$	$4^3\times8$	Z_V^L	Fit	δ_G (%)	Z_V^L	Fit	δ_G (%)
$\beta=8.85$, $a^{-1}=2523$ GeV, $L^*/a=10092$									
0.6	1.3125(17)	1.3578(14)	1.3554(05)	1.3507(43)	1.3485	0.2	1.3507(43)	1.3495	0.1
0.7	1.1812(06)	1.1870(09)	1.1862(07)	1.1846(29)	1.1822	0.2	1.1846(29)	1.1820	0.2
0.8	1.0839(05)	1.0798(09)	1.0787(09)	1.0764(34)	1.0764	0.0	1.0764(34)	1.0755	0.1
0.9	1.0175(03)	1.0122(05)	1.0101(03)	1.0060(28)	1.0089	0.3	1.0060(28)	1.0078	0.2
1.0	0.9745(03)	0.9710(05)	0.9701(03)	0.9684(18)	0.9688	0.04	0.9684(18)	0.9675	0.1
1.1	0.9545(05)	0.9522(07)	0.9514(03)	0.9499(19)	0.9503	0.04	0.9499(19)	0.9490	0.1
1.2	0.9553(02)	0.9549(04)	0.9525(03)	0.9476(31)	0.9510	0.4	0.9476(31)	0.9500	0.3
1.3	0.9719(05)	0.9739(08)	0.9728(05)	0.9706(24)	0.9712	0.1	0.9706(24)	0.9705	0.01
1.4	1.0066(03)	1.0155(04)	1.0160(05)	1.0169(18)	1.0133	0.4	1.0169(18)	1.0132	0.4
1.5	1.0631(09)	1.0888(07)	1.0864(04)	1.0816(34)	1.0833	0.2	1.0816(34)	1.0841	0.3
1.6	1.1480(25)	1.1988(10)	1.1974(06)	1.1946(32)	1.1928	0.1	1.1946(32)	1.1953	0.1
1.7	1.2848(44)	1.3802(12)	1.3705(09)	1.3513(118)	1.3651	1.0	1.3513(118)	1.3705	1.4
$\beta=21.0$, $a^{-1}=3.6\times10^9$ GeV, $L^*/a=1.44\times10^{10}$									
0.4	1.5109(34)	1.7583(07)	1.7420(06)	1.7095(197)	1.73370	1.4	1.7095(197)	1.7347	1.5
0.5	1.3605(17)	1.4332(06)	1.4284(03)	1.4176(65)	1.42541	0.6	1.4176(65)	1.4257	0.6
0.6	1.2319(05)	1.2439(04)	1.2430(02)	1.2412(16)	1.24099	0.02	1.2412(16)	1.2410	0.02
0.7	1.1323(01)	1.1263(03)	1.1254(03)	1.1234(16)	1.12412	0.1	1.1234(16)	1.1239	0.05
0.8	1.0599(03)	1.0518(02)	1.0510(02)	1.0494(12)	1.04943	0.0	1.0494(12)	1.0492	0.02
0.9	1.0131(03)	1.0062(02)	1.0049(01)	1.0025(16)	1.00425	0.2	1.0025(16)	1.0040	0.1
1.0	0.9892(02)	0.9837(02)	0.9829(02)	0.9814(11)	0.98212	0.1	0.9814(11)	0.9818	0.04
1.1	0.9851(02)	0.9817(02)	0.9813(02)	0.9805(9)	0.98019	0.03	0.9805(09)	0.9799	0.1
1.2	1.0004(02)	0.9999(02)	0.9994(01)	0.9985(8)	0.99821	0.03	0.9985(08)	0.9980	0.1
1.3	1.0339(02)	1.0399(02)	1.0393(03)	1.0382(11)	1.03848	0.03	1.0382(11)	1.0384	0.02
1.4	1.0865(04)	1.1072(03)	1.1076(01)	1.1084(9)	1.10660	0.2	1.1084(09)	1.1066	0.2
1.5	1.1600(09)	1.2144(03)	1.2148(04)	1.2154(14)	1.21365	0.1	1.2154(14)	1.2140	0.1
1.6	1.2708(31)	1.3827(04)	1.3822(03)	1.3814(13)	1.38158	0.01	1.3814(13)	1.3824	0.1
1.7	1.4563(47)	1.6713(09)	1.6600(05)	1.6375(137)	1.65782	1.2	1.6375(137)	1.6597	1.4

It has been shown that $Z_V=Z_A$ in perturbation theory for DWQCD at $N_s=\infty$ [14], and as already mentioned in the previous section, this equality is well satisfied nonperturbatively at $\beta=6.0$ for the plaquette action and at $\beta=2.6$ for the RG action. Although violation of this equality becomes larger at stronger coupling (at $\beta=5.8$ for the plaquette action and at $\beta=2.4,2.2$ for the RG action) or at the values of M far away from the ''minimum'' where the chiral symmetry is best realized, we define $Z_A=Z_V$ for DWQCD in this paper, taking numerical values of Z_V as the renormalization factor for both vector and axial-vector currents. Therefore we discuss Z_V only hereafter.

A. Z_V as a function of M

At each g^2, we fit Z_V as a function of M by the formula

$$Z_V^{\rm fit}=\frac{B_0+B_1(M-M_c)+B_2(M-M_c)^2}{1+A_2(M-M_c)^2}, \qquad (22)$$

which is suggested by the perturbation theory [14]. Results for fit parameters M_C, A_2, and $B_i(i=0,1,2)$ are given in Tables IV and V, together with $\delta^{\rm max}$, the maximum of the relative errors δ defined by

$$\delta=(Z_V-Z_V^{\rm fit})/Z_V. \qquad (23)$$

As we observe that $\delta^{\rm max}$ are typically less than 1% and at most a few%, the fit describes data well.

B. Finite a/L errors

Errors of Z_V associated with the lattice spacing are $O((a/L)^2)$ in the $N_s\to\infty$ limit or $O(e^{-\alpha N_s}\times a/L)$ at finite N_s. If $a/L=1/N_l=1/8$ is kept fixed at all values of g^2, the scaling violation in $Z_{V,A}$ remains even in the $g^2\to0$ limit. In order to reduce or remove this scaling violation, we interpolate or extrapolate Z_V to a fixed value of L at each g^2,

TABLE IV. Fit parameters of Z_V as a function of M for the plaquette action.

β	M_c	A_2	B_0	B_1	B_2	$\delta^{\max}$ (%)
			$8^3\times 16\times 16$			
5.8	1.758(14)	−1.441(64)	0.7253(19)	−0.121(30)	−0.263(65)	1.4
6.0	1.661(47)	−1.449(71)	0.7592(55)	−0.088(89)	−0.313(44)	0.2
6.2	1.658(12)	−0.957(46)	0.7762(09)	0.013(22)	0.095(48)	0.2
6.5	1.562(13)	−1.290(14)	0.7985(08)	−0.051(25)	−0.231(11)	0.2
6.8	1.530(14)	−1.478(120)	0.8141(06)	−0.023(25)	−0.416(111)	0.3
7.4	1.483(08)	−1.124(76)	0.8394(06)	0.021(13)	−0.108(76)	0.2
8.0	1.399(01)	−1.066(04)	0.8573(05)	−0.039(01)	−0.033(04)	0.2
9.6	1.319(07)	−1.026(53)	0.8889(05)	−0.015(14)	0.0002(589)	0.1
12.0	1.242(01)	−1.083(19)	0.9167(03)	−0.010(01)	−0.077(24)	0.2
24.0	1.110(01)	−1.058(05)	0.9628(02)	−0.008(02)	−0.068(08)	0.1
			$4^3\times 8\times 16$			
5.8	1.639(11)	−1.570(23)	0.7676(40)	−0.131(26)	−0.267(51)	0.9
			$12^3\times 24\times 16$			
6.0	1.734(14)	−0.899(190)	0.7441(17)	0.0016(251)	0.162(183)	1.0
6.2	1.902(13)	−0.552(03)	0.8228(07)	0.4180(15)	0.389(03)	0.5
6.5	1.607(07)	−1.149(28)	0.7946(09)	0.0217(127)	−0.119(31)	0.3
6.8	1.645(71)	−0.591(128)	0.8191(17)	0.1823(121)	0.391(121)	0.3
7.4	1.486(38)	−0.847(224)	0.8366(11)	0.0221(721)	0.158(211)	0.2
8.0	1.455(08)	−0.931(02)	0.8556(05)	0.0670(14)	0.076(05)	0.1
9.6	1.333(06)	−0.905(57)	0.8871(04)	0.0132(134)	0.108(62)	0.1
12.0	1.252(01)	−1.035(01)	0.9153(02)	0.0103(05)	−0.036(01)	0.1
24.0	1.115(01)	−1.008(04)	0.9617(01)	0.0042(18)	−0.008(06)	0.03

using data on two different spatial lattice sizes L. For the interpolation or the extrapolation, we adopt the linear dependence

$$Z_V(a/L) = Z_V + c\frac{a}{L} = Z_V + c\frac{1}{N_l}. \tag{24}$$

Since only data at two different N_l are available, the value of Z_V at fixed L and its error are estimated by

$$Z_V(a/L) = \frac{Z_V^2 x_1 - Z_V^1 x_2}{x_{12}}, \tag{25}$$

$$\delta Z_V(a/L) = \frac{|\delta Z_V^2 x_1| + |\delta Z_V^1 x_2|}{x_{12}}, \tag{26}$$

where $Z_V^i = Z_V(1/N_i)$, $x_i = 1/N_i - a/L (i=1,2)$, and $x_{12} = 1/N_1 - 1/N_2$ with $N_1 = 8$ and $N_2 = 4$ or 12, and δ means the error of the corresponding quantity. To estimate the systematic uncertainty associated with the assumption, Eq. (24), we alternatively employ the quadratic form

$$Z_V(a/L) = Z_V + c\frac{a^2}{L^2} = Z_V + c\frac{1}{N_l^2}, \tag{27}$$

and calculate $Z_V(1/L)$. A difference in $Z_V(a/L)$ between the linear and the quadratic dependences is quadratically added to $\delta Z_V(a/L)$ as an estimate of the systematic uncertainty, while the central value of $Z_V(a/L)$ is taken from the value obtained from the linear assumption.

In Tables II and III, the values of $Z_V(a/L)$ are given at $L = L^* = 8a(\beta = 6.0)$ (the fifth column), where $a(\beta = 6.0)$ is the lattice spacing at $\beta = 6.0$ for the plaquette action, and at $L = \infty$ (the eighth column). While the former definition of Z_V contains an $O(a/L^*)$ error, which vanishes in the continuum limit, the latter one is free from such an uncertainty. By taking the difference of Z_V between $L = L^*$ and ∞, the a/L^* error in Z_V is estimated to be 0.06 at $M = 1.8$ and $\beta = 6.0$ ($a^{-1} = 2$ GeV) for the plaquette action or 0.02 at $M = 1.7$ and $\beta = 2.6$ ($a^{-1} = 1.9$ GeV) for the RG action. On the other hand, the error associated with the extrapolation in L is larger at $L = \infty$: 0.002 ($L = L^*$) and 0.025 ($L = \infty$) at the previous parameters for the plaquette action and 0.002 and 0.017 for the RG action. Moreover Z_V at $L = \infty$ monotonically decreases as M increases at $a^{-1} < 2$ GeV, while it has the minimum in M at $a^{-1} \geqslant 2$ GeV. Only the latter behavior is observed for Z_V at $L = L^*$. We suspect that the behavior of Z_V at $L = \infty$ is related to the existence of (near) zero eigenvalues

TABLE V. Fit parameters of Z_V as a function of M for the RG action.

β	M_c	A_2	B_0	B_1	B_2	$\delta^{\max}$ (%)
			$8^3\times 16\times 16$			
2.2	1.814(13)	−1.773(75)	0.7125(21)	−0.111(28)	−0.614(98)	1.6
2.4	1.661(15)	−1.469(136)	0.7596(40)	−0.092(28)	−0.394(140)	0.7
2.6	1.577(05)	−1.238(26)	0.7864(09)	−0.053(11)	−0.168(35)	0.3
2.9	1.491(09)	−1.192(03)	0.8226(10)	−0.042(16)	−0.142(10)	0.1
3.2	1.453(06)	−1.318(03)	0.8443(03)	0.005(01)	−0.282(03)	0.1
3.6	1.406(01)	−0.921(81)	0.8664(04)	0.035(02)	0.090(82)	0.1
4.1	1.338(01)	−1.104(04)	0.8856(02)	0.008(01)	−0.100(04)	0.01
4.7	1.290(03)	−0.980(64)	0.9023(04)	0.008(07)	0.031(69)	0.1
6.4	1.213(41)	−1.080(41)	0.9306(03)	0.018(03)	−0.083(45)	0.1
8.85	1.143(01)	−1.058(01)	0.9513(01)	−0.005(01)	−0.068(01)	0.1
21.0	1.062(01)	−1.046(02)	0.9806(01)	0.002(01)	−0.060(04)	0.1
			$4^3\times 8\times 16$			
2.2	1.675(08)	−1.856(141)	0.7618(40)	−0.154(16)	−0.641(144)	3.0
2.4	1.583(16)	−1.556(58)	0.7908(38)	−0.116(40)	−0.377(70)	1.8
			$12^3\times 24\times 16$			
2.6	1.678(07)	−1.017(14)	0.7863(21)	0.098(12)	−0.006(26)	0.6
2.9	1.522(01)	−0.834(84)	0.8170(11)	0.008(03)	0.177(91)	0.3
3.2	1.456(02)	−1.001(12)	0.8401(05)	0.005(04)	0.012(13)	0.2
3.6	1.419(08)	−0.993(03)	0.8643(05)	0.055(01)	0.004(06)	0.1
4.1	1.360(06)	−1.253(65)	0.8832(07)	0.050(11)	−0.245(68)	0.03
4.7	1.314(02)	−1.092(52)	0.9000(04)	0.055(04)	−0.085(56)	0.1
6.4	1.226(02)	−0.893(20)	0.9288(03)	0.044(03)	0.120(23)	0.1
8.85	1.151(01)	−1.003(09)	0.9496(02)	0.012(03)	0.0002(118)	0.03
21.0	1.062(01)	−1.009(01)	0.9797(01)	0.004(01)	−0.011(02)	0.1

for the Hermitian Wilson-Dirac operator at $a^{-1}<2$ GeV: It suggests that the gap of zero eigenvalues for the Hermitian Wilson-Dirac operator is closed at $a^{-1}<2$ for both plaquette and RG actions. This speculation is consistent with the observation that DWQCD cannot realize an exact chiral symmetry even in the $N_s\to\infty$ limit at $a^{-1}\simeq 1$ GeV for both gauge actions [12], though the quenched artifact may explain the observation [17].

TABLE VI. Fit parameters of Z_V as a function of M and g^2.

		Plaquette		RG	
		$L=L^*$	$L=\infty$	$L=L^*$	$L=\infty$
M_c	a_1	−0.5241	−0.9026	-0.6533×10^{-1}	−0.3094
	a_2	−0.1388	−0.2365	-0.3147×10^{-2}	-0.5493×10^{-1}
	a_3	0.5579×10^{-1}	−0.1050	0.3841×10^{-2}	-0.2635×10^{-4}
B_0	a_4	−0.1166	−0.9145	0.1378	−0.3247
	a_5	0.8692×10^{-2}	0.7845×10^{-1}	-0.1046	0.1959×10^{-1}
	a_6	-0.7698×10^{-1}	0.4397×10^{-1}	-0.4000×10^{-2}	0.8526×10^{-3}
A_2	a_7	−0.6437	0	−0.3460	0
	a_8	−0.2754	0	0	0
	a_9	−0.3689	−0.01092	-0.2235×10^{-1}	0
	a_{10}	0.1002	0	0.1019×10^{-1}	0
B_2	a_{11}	−0.9481	0	−0.3613	0

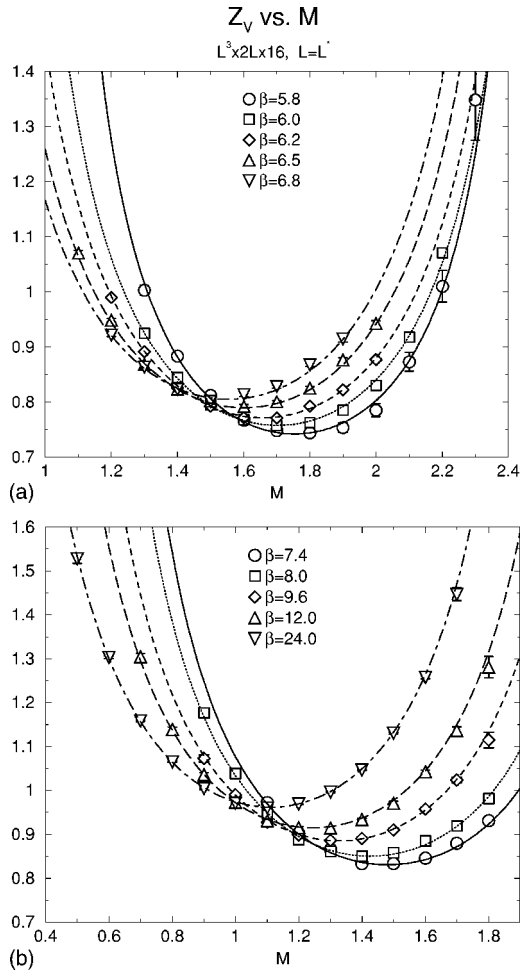

FIG. 5. Z_V as a function M on $L^3\times 2L\times 16$ with $L=L^*$ at several values of β for the plaquette action.

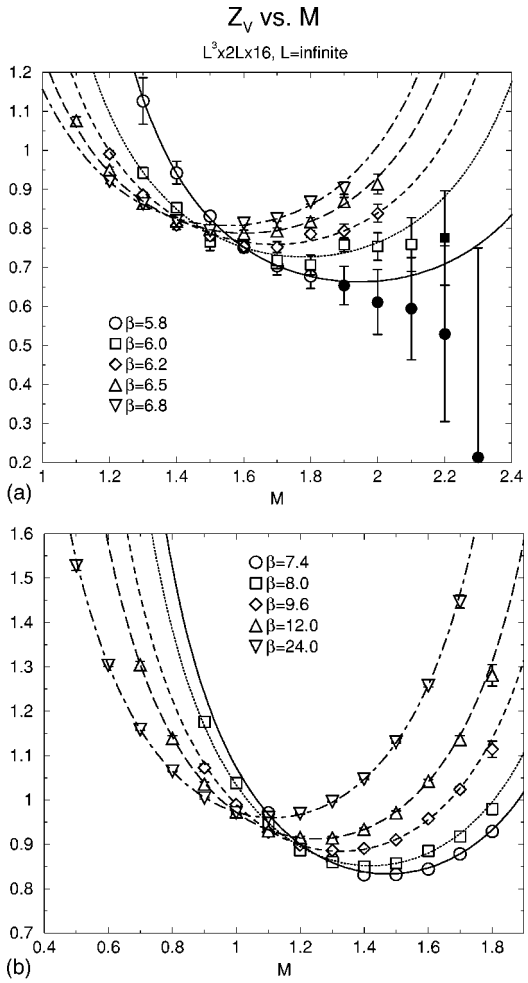

FIG. 6. Z_V as a function M on $L^3\times 2L\times 16$ with $L=\infty$ at several values of β for the plaquette action. Solids symbols are excluded for the fits.

C. Z_V as a function of M and g^2

For the latter uses, we parametrize Z_V as a function of M and g^2, in order to obtain Z at arbitrary (interpolated) values of β and M. We adopt the following fitting function suggested by the perturbation theory [14]:

$$Z_V(g^2,M)=\frac{B_0(g^2)+B_1(g^2)[M-M_c(g^2)]+B_2(g^2)[M-M_c(g^2)]^2}{1+A_2(g^2)[M-M_c(g^2)]^2},$$

$$M_c(g^2)=\frac{1+(c_M+a_1)g^2+a_2g^4+a_3g^6}{1+a_1g^2},$$

$$B_0(g^2)=\frac{1+(c_0+a_4)g^2+a_5g^4+a_6g^6}{1+a_4g^2},$$

$$A_2(g^2)=-\frac{1+(d_2+a_7)g^2+a_9g^4+a_{10}g^6}{1+a_7g^2+a_8g^4},$$

$$B_1(g^2)=c_1g^2,$$

$$B_2(g^2)=\frac{c_2g^2}{1+a_{11}g^2}, \tag{28}$$

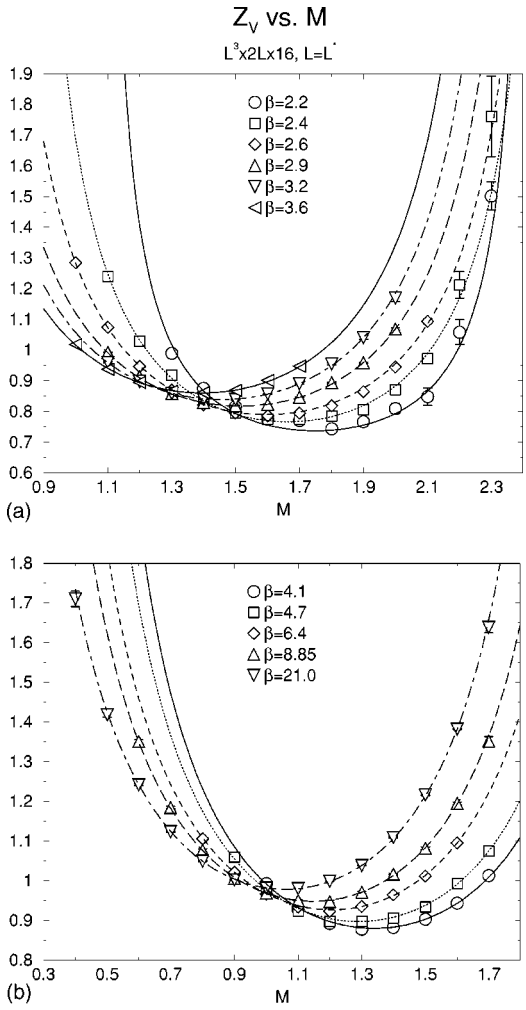

FIG. 7. Z_V as a function M on $L^3\times 2L\times 16$ with $L=L^*$ at several values of β for the RG action.

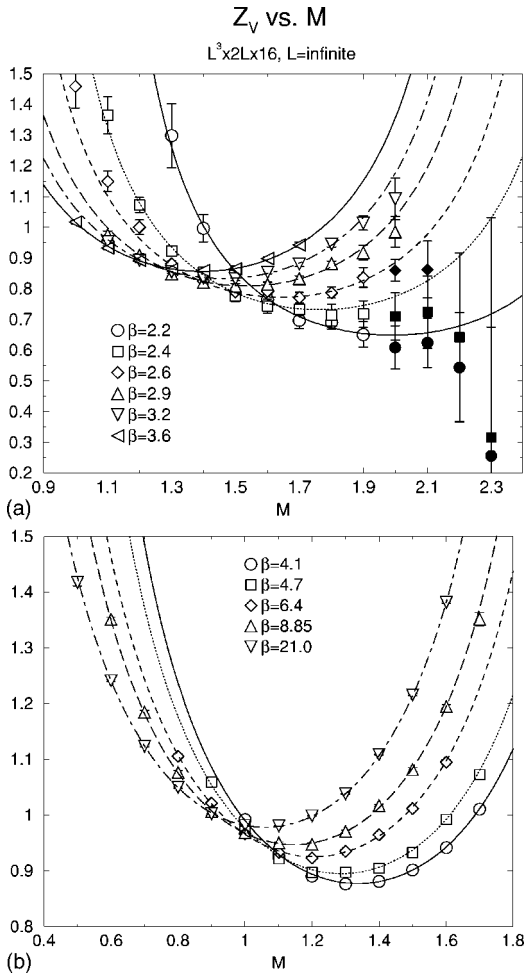

FIG. 8. Z_V as a function M on $L^3\times 2L\times 16$ with $L=\infty$ at several values of β for the RG action. Solids symbols are excluded for the fits.

where c_M, d_2, and $c_i(i=0,1,2)$ are values of one-loop coefficients for M_c, A_2, and $B_i(i=0,1,2)$ [14], which are given by

$$(c_M,d_2,c_0,c_1,c_2)=(0.4177,0.01173,-0.1456,2.311\times 10^{-3},-5.172\times 10^{-3})$$

for the plaquette action and

$$(c_M,d_2,c_0,c_1,c_2)=(0.2070,8.131\times 10^{-3},-0.07449,1.912\times 10^{-3},-4.154\times 10^{-3})$$

for the RG action. These constraints make M_c, A_2, and $B_i(i=0,1,2)$ consistent with the perturbation theory at one loop. Numerical values of the parameters $a_i(i=1-11)$ are given in Table VI for both $L=L^*$ and $L=\infty$. In order to show the quality of the fits, we plot the fitting curves for $Z_V(a/L^*)$ and $Z_V(0)$ in Figs. 5 and 6 for the plaquette action and in Figs. 7 and 8 for the RG action, respectively. Furthermore, we compile $Z_V(g^2,M)$ and the relative deviation

$$\delta_G=\frac{Z_V-Z_V(g^2,M)}{Z_V} \tag{29}$$

in the sixth and seventh columns or the ninth and tenth columns of Tables II and III, where $Z_V=Z_V(a/L^*)$ or $Z_V(0)$, respectively. In the fit for $Z_V(0)$ we exclude a few points for larger values of M at $\beta=5.8$ and 6.0 for the plaquette action and at $\beta=2.2,2.4,2.6$ for the RG action, which are represented by solid symbols in the figures and are marked by "-" in the tables. These data for $Z_V(0)$ have large errors and large values of δ_G. Note however that data excluded for the fit are consistent with the fitting curves within large errors. From the figures and tables we observe that the fits works well and δ_G are less than a few %, except a few points at the edges of the range in M employed for the simulations.

We finally investigate how accurate the perturbative estimation for Z_V at one loop [14] is, by considering a relative error,

$$\delta_{1\text{-loop}}=\frac{Z_V(1\text{-loop})-Z_V(\text{nonperturbative})}{Z_V(\text{nonperturbative})}, \qquad (30)$$

at $M=M_c(g^2)$ as a function of g^2. We then define $g_c^2(3\%)$ such that $\delta_{1\text{-loop}}\leqslant 0.03$ at $g^2\leqslant g_c^2(3\%)$, where g^2 is the bare coupling constant. We find $g_c^2(3\%)\simeq 0.6(1.0)$ in naive perturbation theory or $g_c^2(3\%)\simeq 1.0(1.8)$ in mean-field-improved perturbation theory for the plaquette (RG-improved) gauge action. Although $g_c^2(3\%)$ is smaller for the plaquette action, the corresponding lattice spacing a is larger than that for the RG-improved action. In particular, the MF-improved perturbation theory works well even at $\beta=6.0(a\simeq 0.1$ fm) for the plaquette action.

VI. CONCLUSIONS AND DISCUSSIONS

We calculate the renormalization factors for the vector and axial-vector currents in the quenched DWQCD for both plaquette and RG actions. After several tests are performed at $a^{-1}\simeq 2$ GeV, we obtain Z_V, which is assumed to be equal to Z_A, at $L=\infty$ as well as $L=L^*$ for the wide ranges of g^2 and M. We globally fit Z_V as a function of g^2 and M.

We now propose how to use these results for the future simulations of the quenched DWQCD.

(i) For the DWQCD to realize the chiral symmetry well, one should take at least $a^{-1}\geqslant 2$ GeV. This condition is satisfied at $\beta\geqslant 6.0$ for the plaquette action or at $\beta\geqslant 2.6$ for the RG action.

(ii) One should choose the optimal value of M, which minimizes the violation of the chiral symmetry at finite N_s. A good candidate is the choice that $M\simeq M_c(g^2)$, where

$$M_c(g^2)=\frac{1+(c_M+a_1)g^2+a_2g^4+a_3g^6}{1+a_1g^2}. \qquad (31)$$

The parameters $a_{1,2,3}$ are given in Table VI.

(iii) If the simulation point at g^2 and M can be found in Table II or III, one should use Z_V in the table as the renormalization factor for the vector or axial-vector current. To remove $O(a/L)$ errors in Z_V, it is better to take Z_V at $L=\infty$, though the statistical error of Z_V is larger in this case. One may use Z_V at $L=L^*$ to estimate the size of $O(a/L)$ errors in Z_V.

(iv) If g^2 or M for the simulation point is not found in the tables, one should use the fitting function given in Eq. (28) with the parameters in Table VI. The error of Z_V is estimated from the errors of Z_V at the nearest points in g^2 and M, which can be found in the tables.

We are encouraged by the present results to proceed to an extension of the present work to scale-dependent cases such as quark masses and four-quark operators needed for B_K, implementing the SF boundary condition for the domain-wall fermions [10].

ACKNOWLEDGMENTS

S.A. thanks Professor M. Lüscher, Professor S. Sint, Professor P. Weisz, and Professor H. Wittig for useful discussions. This work is supported in part by Grants-in-Aid from the Ministry of Education (Nos. 12304011, 12640253, 12740133, 13135204, 13640259, 13640260, 14046202, 14740173, 15204015, 15540251, 15540279, 15740134).

[1] CP-PACS Collaboration, A. Ali Khan *et al.*, Phys. Rev. D **64**, 114506 (2001).

[2] G. Maritinelli *et al.*, Nucl. Phys. **B445**, 81 (1995); A. Donini *et al.*, Phys. Lett. B **360**, 83 (1995); V. Gimenez *et al.*, Nucl. Phys. **B531**, 429 (1998); D. Becirevic *et al.*, Phys. Lett. B **444**, 401 (1998); M. Göckeler *et al.*, Nucl. Phys. **B544**, 699 (1999); A. Donini *et al.*, Eur. Phys. J. C **10**, 121 (1999); S. Aoki *et al.*, Phys. Rev. Lett. **82**, 4392 (1999); L. Guisti and A. Vladikas, Phys. Lett. B **488**, 303 (2000).

[3] M. Lüscher *et al.*, Nucl. Phys. **B384**, 168 (1992); K. Jansen *et al.*, Phys. Lett. B **372**, 275 (1996); M. Lüscher *et al.*, Nucl. Phys. **B478**, 365 (1996); M. Lüscher *et al.*, *ibid.* **B491**, 344 (1997); S. Capitani *et al.*, *ibid.* **B544**, 669 (1999).

[4] T. Blum *et al.*, Phys. Rev. D **66**, 014504 (2002).

[5] Y. Iwasaki, Nucl. Phys. **B258**, 141 (1985); University of Tsukuba Report No. UTHEP-118, 1983.

[6] Recently c_t for the RG action has been calculated at one loop: S. Takeda, S. Aoki, and K. Ide, Phys. Rev. D **68**, 014505 (2003).

[7] S. Aoki, R. Frezzotti, and P. Weisz, Nucl. Phys. **B540**, 501 (1999).

[8] Y. Shamir, Nucl. Phys. **B406**, 90 (1993); V. Furman and Y. Shamir, *ibid.* **B439**, 54 (1995).

[9] S. Sint, Nucl. Phys. **B421**, 135 (1994). See also S. Sint, Nucl. Phys. B (Proc. Suppl.) **94**, 79 (2001).

[10] S. Aoki, Y. Kikukawa, and Y. Taniguchi (in preparation).

[11] M. Lüscher and P. Weisz, Nucl. Phys. **B479**, 429 (1996).

[12] CP-PACS Collaboration, A. Ali Khan *et al.*, Phys. Rev. D **63**, 114504 (2001).

[13] S. Aoki, T. Izubuchi, Y. Kuramashi, and Y. Taniguchi, Phys. Rev. D **62**, 094502 (2000).

[14] S. Aoki, T. Izubuchi, Y. Kuramashi, and Y. Taniguchi, Phys. Rev. D **59**, 094505 (1999); **67**, 094502 (2003).

[15] C. Allton, hep-lat/9610016; Nucl. Phys. B (Proc. Suppl.) **53**, 867 (1997).

[16] M. Okamoto *et al.*, Phys. Rev. D **60**, 094510 (1999).

[17] M. Golterman and Y. Shamir, Phys. Rev. D **68**, 074501 (2003).